BMC Cardiovascular Disorders

RESEARCH

Open Access

Magnetic resonance imaging quantification of left ventricular mechanical dispersion and scar heterogeneity optimize risk stratification after myocardial infarction

Xiaoying Zhao[1†], Li Zhang[1†], Lujing Wang[1], Wanqiu Zhang[1], Yujiao Song[1], Xinxiang Zhao[1*] and Yanli Li[2]

Abstract

Background Left ventricular (LV) myocardial contraction patterns can be assessed using LV mechanical dispersion (LVMD), a parameter closely associated with electrical activation patterns. Despite its potential clinical significance, limited research has been conducted on LVMD following myocardial infarction (MI). This study aims to evaluate the predictive value of cardiac magnetic resonance (CMR)-derived LVMD for adverse clinical outcomes and to explore its correlation with myocardial scar heterogeneity.

Methods We enrolled 181 post-MI patients (median age: 55.7 years; 76.8% male) who underwent CMR examinations. LVMD was calculated using the CMR-feature tracking (CMR-FT) technique, defined as the standard deviation (SD) of the time from the R-wave peak to the negative strain peak across 16 myocardial segments. Entropy was quantified using an algorithm implemented with a generic Python package. The primary composite endpoints included sudden cardiac death (SCD), sustained ventricular arrhythmias (VA), and new-onset heart failure (HF).

Results Over a median follow-up of 31 months, LVMD and border zone (BZ) entropy demonstrated relatively high accuracy for predicting the primary composite endpoints, with area under the curve (AUC) values of 0.825 and 0.771, respectively. Patients with LVMD above the cut-off value (86.955 ms) were significantly more likely to experience the primary composite endpoints compared to those with lower LVMD values ($p < 0.001$). Multivariable analysis identified LVMD as an independent predictor of the primary composite endpoints after adjusting for entropy parameters, strain, and left ventricular ejection fraction (LVEF) (hazard ratio [HR]: 1.014; 95% confidence interval [CI]: 1.003–1.024; $p = 0.010$). A combined prediction model incorporating LVMD, BZ entropy, and LVEF achieved the highest predictive accuracy, with an AUC of 0.871 for the primary composite endpoints. Spearman rank correlation analysis revealed significant linear correlations between LVMD and entropy parameters ($p < 0.001$ for all).

†Xiaoying Zhao and Li Zhang contributed equally to this work and should be considered as co-first authors.

*Correspondence:
Xinxiang Zhao
zhaoxinxiang2918@outlook.com

Full list of author information is available at the end of the article

Conclusions Myocardial heterogeneity, as assessed by LVMD and BZ entropy, represents reliable and reproducible parameters reflecting cardiac remodeling following MI. LVMD has independent prognostic value, and the combination of LVMD and BZ entropy with the guideline-recommended LVEF as a unified model enhances the accuracy of forecasting the risk of primary combined endpoints in patients after MI.

Keywords Mechanical dispersion, Entropy, Myocardial infarction, Ventricular remodeling, Cardiac magnetic resonance

Introduction

According to the Annual Report on Cardiovascular Health and Diseases in China (2021), cardiovascular disease is one of the largest single causes of death among Chinese residents. The incidence of myocardial infarction (MI) is rising, with a growing trend among younger individuals. This increase in hospitalization and mortality rates has become a significant medical and societal challenge, profoundly impacting people's health and quality of life [1]. Although the widespread adoption of percutaneous coronary intervention (PCI) technology has significantly lowered MI-related mortality, the long-term prognosis for MI patients remains poor. Patients with MI face an increased risk of primary combined endpoints due to the gradual and extensive loss of myocardial tissue post-infarction, accompanied by structural and electrophysiological remodeling, which can lead to heart failure (HF) and sustained ventricular arrhythmias (VA) [2].

The current guidelines recommend implanting implantable cardioverter defibrillator (ICD) to prevent sudden cardiac death (SCD) in post-MI patients with New York Heart Association (NYHA) class II–III and reduced left ventricular ejection fraction (LVEF) < 35%. For NYHA class I patients, ICD therapy should be considered if LVEF ≤ 30%. In addition, ICD implantation is recommended for patients with LVEF ≤ 40% despite ≥ 3 months of optimal medical therapy and non-sustained ventricular tachycardia (NSVT), if they are inducible for sustained monomorphic ventricular tachycardia (SMVT) by programmed electrical stimulation (PES) [3]. However, recent studies have demonstrated that screening patients for ICD placement based on a single metric of LVEF is not ideal, as a recent multicenter study showed that 875 (13%) of 6822 patients with LVEF ≥ 35% developed primary combined endpoints over a median follow-up of 707 days [4].

Cardiac magnetic resonance (CMR) is the gold standard imaging technique for assessing myocardial remodeling after myocardial infarction (MI). Most current studies emphasize myocardial fibrosis, primarily evaluated through late gadolinium enhancement (LGE). LGE entropy, which has emerged in recent years, is a new parameter that reflects the tissue and structural heterogeneity of fibrotic regions of myocardial ischemic injury [5]. Based on varying levels of ischemia and pathophysiological distinctions, the ventricular myocardium is categorized into three regions: the infarct core (IC), the border zone (BZ), and the remote non-infarcted myocardium. BZ, which consists of a mixture of surviving myocardium and fibrous tissue, increases the degree of inhomogeneous anisotropy. This leads to a heightened risk of electrolytic coupling, the formation of regions with conduction block and slow conduction, thereby creating a favorable environment for the development of sustained VA [6]. These three regions can be Identified on LGE images, and entropy values can reflect the regional structural heterogeneity.

Since the LV myocardial contraction pattern correlates with its electrical activation pattern, this apparent inhomogeneous activation can be detected through left ventricular mechanical dispersion (LVMD) [7]. However, research on LVMD following MI remains limited, with most existing studies relying on echocardiographic evaluations [8]. CMR allows highly reproducible tracking of myocardial deformation, making it more suitable than echocardiography for LVMD evaluation [9]. A study in 2016 showed that LVMD not only reflects electrophysiologic remodeling, but also has a association with myocardial fibrosis, with increased LVMD correlating with the degree of myocardial fibrosis observed with CMR [10]. The aim of this study was to investigate the predictive value of CMR-derived LVMD for outcomes after MI, as well as its correlation with LGE entropy.

Methods

Study population

For this retrospective study, consecutive participants (age > 18 years) with previous MI more than 3 months ago were recruited between September 2017 and August 2022. Inclusion criteria were: (a) previous MI, immediate coronary angiography showing ≥ 70% stenosis in ≥ 1 coronary artery or ≥ 50% stenosis of the left main stem, (b) had undergone CMR examination 3–6 months after MI and myocardial scar in an ischaemic distribution (subendocardial or transmural hyperintensity distributed in the coronary supply territory), and (c) NYHA class ≤ III. Exclusion criteria were: (a) myocardial scar due to another original and secondary cardiomyopathy, or (b) history of VAs, or (c) any contraindication to CMR, or (d) poor CMR image quality, or (e) incomplete clinical data.

The primary combined endpoints were defined as the combination of SCD, sustained VA or/and ICD

implantation, and newly emerging heart failure (CHF). SCD was defined as sudden death of cardiac origin, occurring within 1 h of the onset of symptoms in a witnessed case and within 24 h of the last surviving case. Death records with medical records were required. VAs for this analysis referred to the occurrence of a first SVT or VF event [11]. Patients underwent ICD therapy at the discretion of the cardiologist based on current guidelines. New CHF was determined as the first episode of cardiac decompensation requiring hospital re-admission.

The outcome data were collected from patients or first-degree relatives and hospitalization records. Demographics, echocardiography, and relevant medical examination data were determined by an investigator (SY.J.) blinded to CMR information up to October 2023. The study complied with the Declaration of Helsinki and was approved by the Chinese Clinical Trial Registry (https://www.chictr.org.cn, Registration ID: ChiCTR2200055158, registration date: January 2, 2022), written informed consents were obtained from all participants.

CMR images acquisition

All images were acquired with a 3.0-T MR scanner (Achieva, Philips Medical System, the Netherlands) using an 18-channel body phased-array surface coil together with electrocardiographic gating techniques. High-resolution cine images of short-axis (SAX), 2-chamber, 3-chamber, and 4-chamber long-axis were performed using steady-state free precession sequence with repetition time (TR)=3.1 ms, echo time (TE)=1.54ms, flip angle (FA)=45°, temporal resolution=40 ms, slice thickness=8 mm, field of view (FOV)=350 mm×350 mm, and voxel size=1.8 mm×1.4 mm×8.0 mm. LGE images were obtained at 15 min after a bolus injection of contrast agent gadoteridol (Gd-HP-DO3A, ProHance, BIPSO GmbH, Berlin, Germany) at a dose of 0.1mmol/kg with a flow rate of 2.5mL/s. LGE images were optimized using an inversion recovery gradient-echo imaging sequence, and the imaging parameters were as follows: TR=5.0msec, TE=2.4msec, FA=25°, slice thickness=6 mm, FOV: 320 mm×320 mm, and voxel size=1.8 mm×1.4 mm×8.0 mm.

LV strain analysis

All image post-processing procedures were performed using the commercially available post-processing software CVI 42 (Circle Cardiovascular Imaging Inc®, v5.1.4, Calgary, Canada). The endocardium and epicardium of SAX, 2-chamber, 3-chamber and 4-chamber long-axis images were tracked using a semi-automated tracking algorithm throughout the entire cardiac cycle. To ensure accuracy of the endocardial and epicardial contours, the performance of the software was visually reviewed by observers and manually adjusting the contours if necessary.

The definition of end-diastole relies on the closure time of the mitral valve. Functional parameter LVEF, LV end-diastolic volume index (LVEDVI), LV end-systolic volume index (LVESVI) were automatic acquisition via standard volumetric techniques on pre-contoured SAX images. Cardiac index (CI) was calculated by cardiac output (CO) /body surface area (BSA) as defined in a previous study [12].

Three-dimensional (3D) feature tracking analysis was automatically performed using the 'strain' module in pre-contoured SAX, 2-chamber, 3-chamber, and 4-chamber long-axis images. All contours were initially assessed using a visual estimation to ensure accurate tracking of the left ventricular wall. Manual adjustments were made when necessary. The software algorithm automatically calculated 3D peak strains, subsequently the global strain parameters including global radial strain (GRS), global circumferential strain (GCS), and global longitudinal strain (GLS) were automatically acquired by averaging the peak values of the 16 segments. Global systolic radial strain rate (GRSRd), global systolic circumferential strain rate (GCSRd), global systolic longitudinal strain rate (GLSRd), global diastolic radial strain rate (GRSRd), global diastolic circumferential strain rate (GCSRd), global diastolic longitudinal strain rate (GLSRd) values were acquired as the mean of all segmental strain rate. LVMD was defined as the standard deviation (SD) of the time from the peak of the R wave and the negative 3D strain peak in 16 segments and can be generated automatically by the software (Fig. 1). This strain analysis was undertaken by two separate observers (XY.Z., and L.Z.) who had more than 3 years of CMR experience and were blinded to patients' clinical data.

Infarct quantification and entropy calculation

LV endocardial and epicardial borders were manually delineated in SAX for detection and quantification of infarct areas. Normal myocardium was manually delineated sufficiently far from the infarct area for reference. LGE segments containing infarction areas were defined using the SDs approach. The signal intensity (SI) thresholds of over 3 SDs and over 2 SDs were chosen, 3 for IC, 2 for entire infarct-related myocardium (BZ+IC, expressed as IBZ), between 2SDs and 3SDs for BZ. After applying semi-automated infarct area detection and performing a visual accuracy review, manual adjustments were made as required.

Entropy calculation was performed using the algorithm executed in Python (MathWorks, version 3.8, Natick, MA). With the use of the CVI 42 workstation, SAX LGE images in infarcted layers with endocardial and epicardial borders as well as labeling of infarct areas were

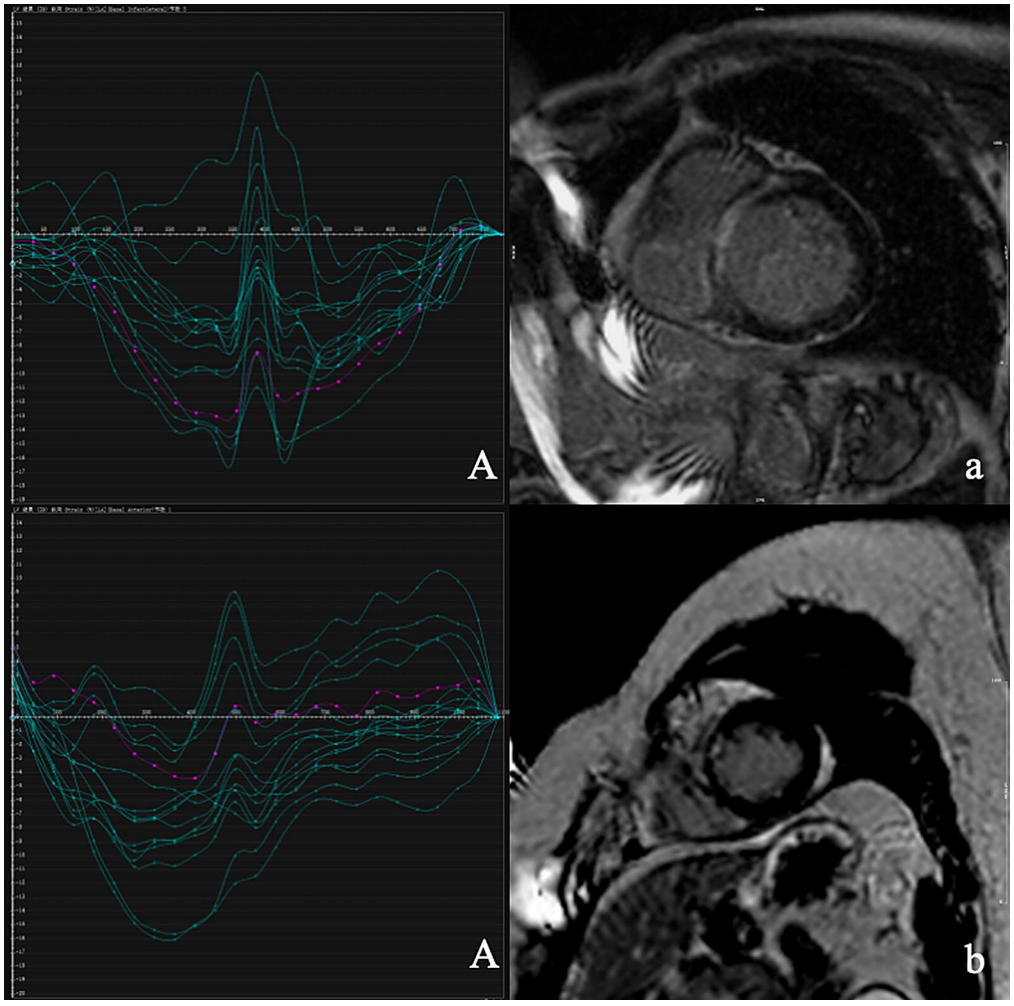

Fig. 1 LVMD (**A and B**, the horizontal axis is time and the vertical axis is strain) and LGE extent of patients (**a and b**), A and a for patient 1, B and b for patient 2. Patient 1, male, 52 years old, LVMD = 92ms, BZ%=7.62%, IC%=20.80%, IBZ%=28.42%, respectively. During the 29-month follow-up period, patients developed VA. Patient 2, male, 47 years old, LVMD = 33ms, BZ%=2.67%, IC%=8.83%, IBZ%=11.50%, respectively. During the 34-month follow-up period, no endpoint events occurred

exported in DICOM format. Meanwhile, original images in the same layers were exported without any labeling in DICOM format. An automated procedure was used to obtain SI per voxel of the myocardium, and the formula below was used to calculate entropy [13]. For the purpose of assessing the reliability of infarct quantification and entropy calculation, all patients were assessed separately by XY.Z., and L.Z. who were blinded to the demographic information, baseline, and outcome data.

Statistical analysis

Statistical analyses were performed using SPSS (version 25, Chicago IL, USA), R software (version 4.0.2, Vienna, Austria), Prism GraphPad (version 9.3.1, La Jolla, CA, USA), and MedCalc (version 20.1.0, Ostend, Belgium). Continuous data were expressed as mean ± SD or median (interquartile range, (IQR)) according to the normality of frequency distribution, evaluated using Shapiro-Wilk's test. Categorical data were summarized as frequencies or percentages. Mann–Whitney test was conducted for continuous variables and the Chi-square test or Fisher's exact test was conducted for categorical variables to compare parameters' differences between subgroups. For comparisons of Inter- and intraobserver measurement agreement, the interclass correlation efficiency (ICC) of subjects was calculated. Spearman rank correlation was used to identify correlations between myocardial entropy and LVMD.

In order to validate the prognostic performance of the LVMD, Receiver Operator Characteristic (ROC) curves were drawn to calculate areas under the curve (AUCs). The cumulative incidence of primary combined endpoints during follow-up was estimated with the use of the Kaplan-Meier survival analyses with LVMD above cut-off value versus below, and survival curves were compared with the use of the log-rank test. Univariable and

multivariable Cox proportional hazards regression analysis with stepwise variable selection was used to investigate the association between variabilities and primary combined endpoints risk. For all analyses, a two-sided p-value < 0.05 was considered statistically significant.

Results

Demographic and clinical characteristics

Of 247 post-MI patients screened, a total of 181 patients (median age 55.7 years, 76.8% males) were involved in this study (Fig. 2). According to the prognosis of the median follow-up of 31 months, 42 patients experienced primary combined endpoints. 2 patients died of SCD, 24 developed VAs and among them, 9 received ICD implantation, 16 developed CHF. The subjects were dichotomized into primary combined endpoints (+) and primary combined endpoints (-) groups (Table 1). MI patients in the primary combined endpoints (-) group were more probably with NYHA class I than patients with primary combined endpoints ($p=0.040$). Whereas, there was no statistically significant difference between the two groups in terms of age, gender, BMI, proportion of hyperlipidemia, hypertension, smoking, and diabetes ($p>0.050$ for all). In addition, MI type, culprit arteries, and secondary medical prevention discharge therapy did not significantly differ in the two study groups ($p>0.050$ for all).

CMR parameters

As presented in Table 1, compared with the patients in the primary combined endpoints(-) group, the primary combined endpoints (+) group had higher LVMI, LVEDVI, LVESVI ($p=0.029$, $p=0.008$, and $p<0.001$, respectively) and lower LVEF ($p<0.001$). The results of fibrosis quantification were also different in the two groups. Patients in the primary combined endpoints (+) group were probability of larger IC%, BZ entropy, IC

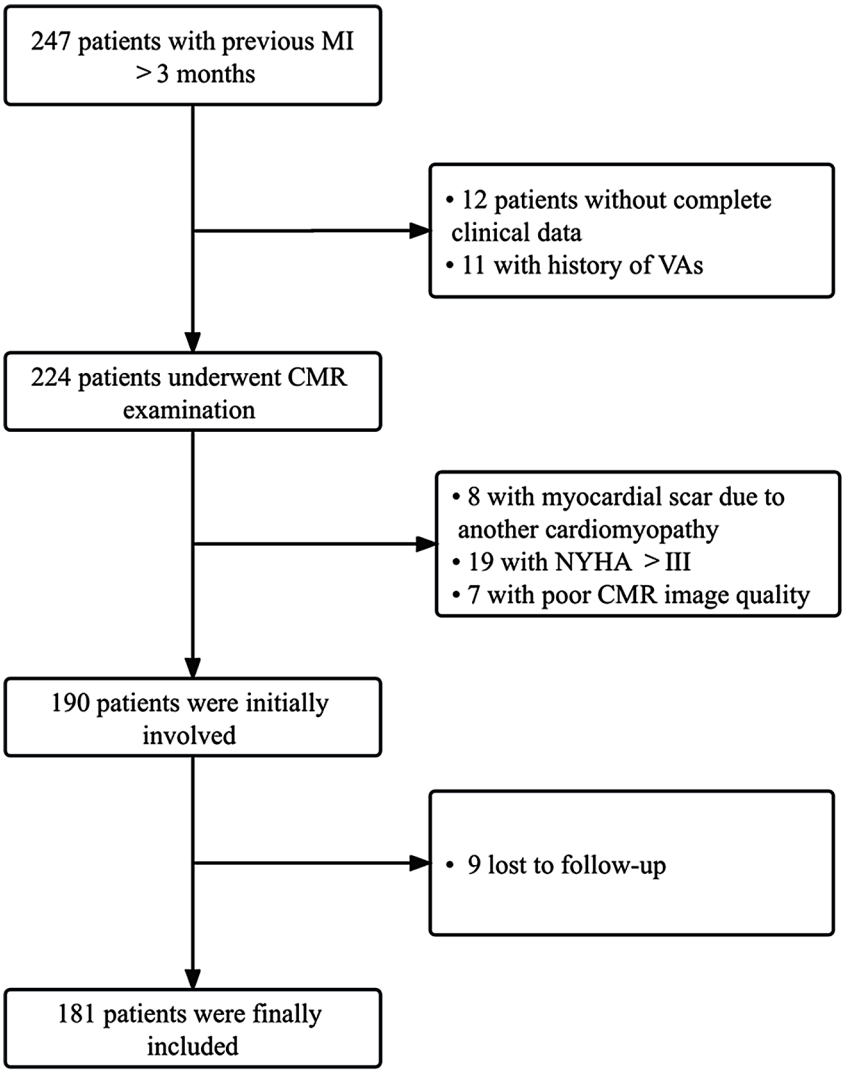

Fig. 2 The flow chart of inclusion and exclusion

Table 1 Baseline characteristics of patients stratified by MACEs

	MACEs (-) ***n*** **= 139**	**MACEs (+)** ***n*** **= 42**	**Z/x/t**	***p*-value**
Age, years	55 ± 14	57 ± 13	0.452	0.652
Male (n %)	106(76.3)	33(78.6)	0.097	0.756
BMI, kg/m^2	23.774(5.028)	23.529(3.106)	-0.084	0.933
CI, L/(min·m^2)	2.309(1.192)	2.124(0.878)	-0.971	0.332
LVMI, g/m^2	55.245(18.960)	62.083(20.556)	-2.184	0.029*
LVEDVI, mL/m^2	77.175(35.494)	93.057(64.058)	-2.655	0.008*
LVESVI, mL/m^2	40.144(32.496)	58.855(56.232)	-3.885	<0.001*
LVEF, %	45.702(21.631)	35.281(20.525)	-4.204	<0.001*
LVEF < 35% (n %)	24(17.3)	20(47.6)	16.150	<0.001*
BZ, %	4.595(3.895)	4.720(2.820)	-0.899	0.369
IC, %	14.385(19.140)	22.970(19.645)	-2.117	0.034*
IBZ, %	20.205(23.875)	28.790(21.366)	-1.949	0.051
BZ entropy	4.452 ± 0.750	5.203 ± 0.736	5.709	<0.001*
IC entropy	6.435(1.135)	6.980(0.683)	-2.485	0.013*
IBZ entropy	6.575(1.330)	6.800(0.863)	-2.274	0.023*
LV entropy	6.030(2.030)	6.600(1.315)	-2.763	0.006*
GRS, %	22.145(14.485)	16.780(14.670)	-2.574	0.010*
GCS, %	-14.369 ± 5.214	-12.394 ± 4.974	2.174	0.031*
GLS, %	-10.107 ± 3.392	-7.977 ± 2.872	3.689	<0.001*
GRSRs, %	1.375(1.490)	1.090(0.865)	-2.509	0.012*
GCSRs, %	-0.825(0.385)	-0.740(0.343)	-2.806	0.005*
GLSRs, %	-0.610(0.385)	-0.570(0.370)	-1.600	0.010*
GRSRd, %	-1.250(1.270)	-1.090(1.165)	-1.106	0.269
GCSRd, %	0.710(0.465)	0.580(0.455)	-2.712	0.007
GLSRd, %	0.605(0.445)	0.500(0.378)	-0.839	0.402
LVMD, ms	68.195(25.040)	98.560(49.753)	-6.379	<0.001*
MI type (n %)			0.627	0.429
STEMI	92(66.2)	25(59.5)		
NSTEMI	47(33.8)	17(40.5)		
Culprit arteries (n %)			0.572	0.751
LAD	75(54.0)	22(52.4)		
LCX	41(29.5)	11(26.2)		
RCA	23(16.6)	9(21.4)		
NYHA class (n %)				
I	68(48.9)	13(31.0)	4.212	0.040*
II	61(43.9)	24(57.1)	2.276	0.131
III	10(7.2)	5(11.9)	0.936	0.344
Hyperlipidemia (n %)	99(71.2)	31(73.8)	0.107	0.744
Hypertension (n %)	93(66.9)	30(71.4)	0.303	0.582
Smoking (n %)	93(66.9)	28(66.7)	0.001	0.977
Diabetes (n %)	58(41.7)	22(52.4)	1.485	0.223
Secondary medical prevention discharge therapy				
Beta-blockers	99(71.2)	31(73.8)	0.107	0.744
RAAS-inhibitors	118(84.9)	36(85.7)	0.030	0.862
Statins	109(78.4)	33(78.6)	0.000	0.983
Loop diuretics	28(20.1)	8(19.0)	0.024	0.876

Values are expressed as mean ± SD, n (%), or median (IQR). *$p < 0.05$ is accepted as statistically significant. BMI, body mass index; CO, cardiac output; CI, cardiac index; TC, total cholesterol; TG, triglyceride; HDL, high density lipoprotein; LDL, low density lipoprotein; LVMI, Left ventricular mass index; LVEDVI, left ventricular end-diastolic volume index; LVESVI, left ventricular end-systolic volume index; LVEF, left ventricular ejection fraction; BZ, border zone; IC, infarct zone; IBZ, infarct zone and border zone; GRS, global radial strain; GCS, global circumferential strain; GLS, global longitudinal strain; GRSRs, global radial strain of systolic rate; GCSRs, global circumferential strain of systolic rate; GLSRs, global longitudinal strain of systolic rate; GRSRd, global radial strain of diastolic rate; GCSRd, global circumferential strain of diastolic rate; GLSRd, global longitudinal strain of diastolic rate; LVMD, left ventricular mechanical dispersion; MI, myocardial infarction; STEMI, st-segment elevation myocardial infarction; NSTEMI, non-st-segment elevation myocardial infarction;,LAD, left anterior descending branch; LCX, left circumflex artery; RAD, right coronary artery; NYHA, New York Heart Association; RAAS, renin-angiotensin-aldosterone system

Table 2 Intra- and interobserver reproducibility statistics for entropy and LVMD measurements

	Intraobserver reproducibility (Observer 1)			Intraobserver reproducibility (Observer 2)			Interobserver reproducibility		
	ICC	95% Limits of agreement	*p*-value	ICC	95% Limits of agreement	*p*-value	ICC	95% Limits of agreement	*p*-value
BZ entropy	0.920	(0.893,0.940)	<0.001*	0.913	(0.884,0.935)	<0.001*	0.884	(0.842,0.915)	<0.001*
IC entropy	0.931	(0.907,0.949)	<0.001*	0.927	(0.903,0.946)	<0.001*	0.892	(0.855,0.919)	<0.001*
IBZ entropy	0.955	(0.939,0.966)	<0.001*	0.956	(0.941,0.968)	<0.001*	0.917	(0.890,0.939)	<0.001*
LV entropy	0.964	(0.952,0.974)	<0.001*	0.973	(0.964,0.980)	<0.001*	0.956	(0.939,0.967)	<0.001*
LVMD	0.984	(0.978,0.988)	<0.001*	0.982	(0.975,0.987)	<0.001*	0.955	(0.937,0.967)	<0.001*

*$p<0.05$ is accepted as statistically significant. Observer 1: XY.Z. Observer 2: L.Z

LVEF, left ventricular ejection fraction; BZ, border zone; IC, infarct zone; IBZ, infarct zone and border zone; GRS, global radial strain; GCS, global circumferential strain; GLS, global longitudinal strain; LVMD, left ventricular mechanical dispersion

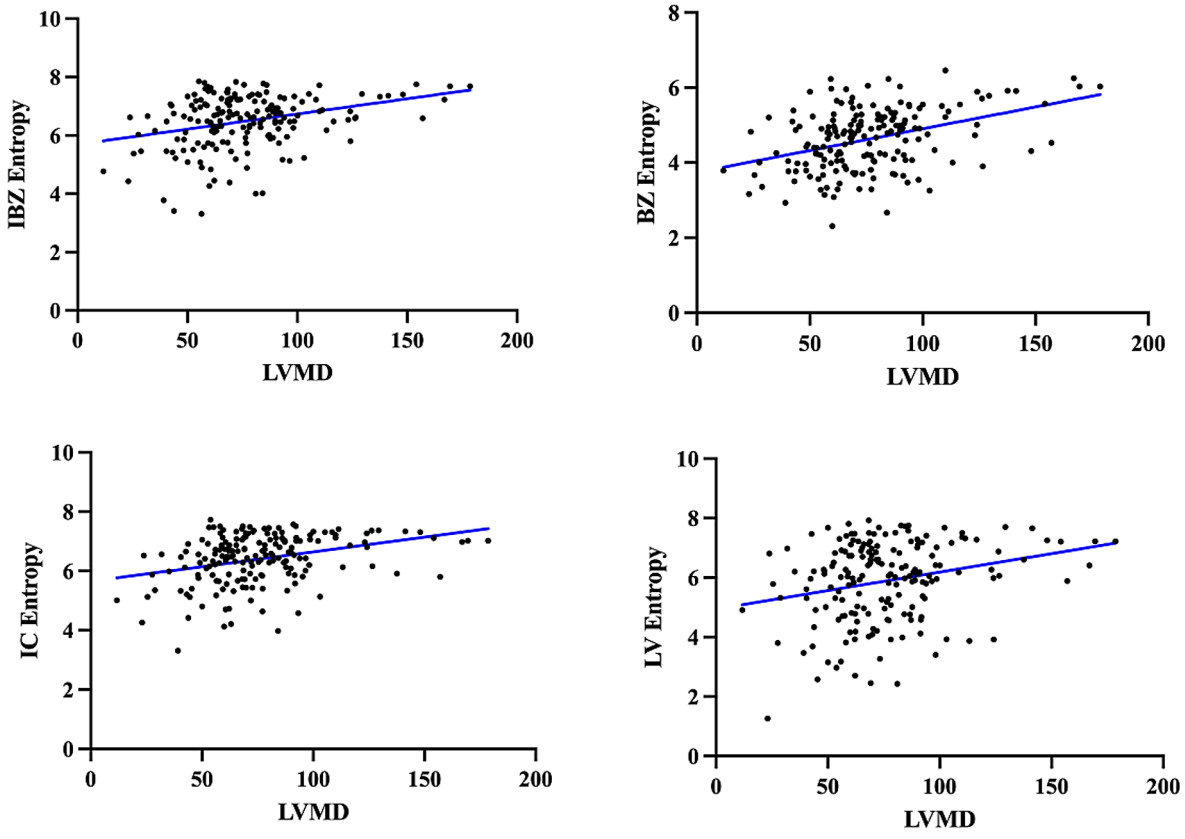

Fig. 3 The results of the spearman rank correlation coefficient showed a linear correlation between LVMD and entropy parameters. BZ entropy ($r=0.397$, $p<0.001$), IC entropy ($r=0.327$, $p<0.001$), IBZ entropy ($r=0.313$, $p<0.001$), LV entropy ($r=0.257$, $p<0.001$)

entropy, IBZ entropy, and LV entropy ($p=0.034$, $p<0.001$, $p=0.013$, $p=0.023$, and $p=0.006$, respectively). As for strain parameters, significant differences of LVMD, GRS, GCS, and GLS ($p<0.001$, $p=0.010$, $p=0.021$, and $p<0.001$, respectively) were found between two groups. Differences of global strain in three directions of systolic rate were different ($p=0.012$, $p=0.005$, and $p=0.010$, respectively), but only different in circumferential of diastolic rate ($p=0.007$). Subgroup analyses demonstrated a similar extent of the BZ% and IBZ% ($p>0.050$ for all). Intra- and interobserver reproducibility statistics for entropy and LVMD measurements were shown in Table 2 and demonstrated good consistency.

Correlation of LVMD and entropy

As present in Fig. 3, Spearman rank correlation demonstrated linear relationships between LVMD and CMR measures of myocardial heterogeneity. A 1-increase in the LVMD was associated with an increase of 0.397 in the BZ entropy, and with an increase of 0.327 in the IBZ entropy. IC entropy and LV entropy were marginally associated with LVMD.

Table 3 ROC of CMR parameters for MACE Eveluation

	AUC	Sensitivity	Specificity	Cut-off value	*p*-value
LVEF (%)	0.714	0.662	0.667	39.660	<0.001*
BZ%	0.546	0.786	0.381	3.715	0.354
IC%	0.608	0.738	0.525	15.045	0.028*
IBZ%	0.599	0.762	0.468	17.823	0.046*
BZ entropy	0.771	0.690	0.799	5.005	<0.001*
IC entropy	0.685	0.690	0.698	6.760	<0.001*
IBZ entropy	0.616	0.881	0.353	6.170	0.012*
LV entropy	0.641	0.833	0.432	5.795	0.004*
GRS(%)	0.631	0.777	0.476	15.710	0.008*
GCS(%)	0.617	0.571	0.669	-12.605	0.019*
GLS(%)	0.691	0.667	0.655	-9.270	<0.001*
LVMD(ms)	0.825	0.690	0.835	86.955	<0.001*

*$p<0.05$ is accepted as statistically significant

LVEF, left ventricular ejection fraction; BZ, border zone; IC, infarct zone; IBZ, infarct zone and border zone; GRS, global radial strain; GCS, global circumferential strain; GLS, global longitudinal strain; LVMD, left ventricular mechanical dispersion

Table 4 Univariable and multivariable cox regression analysis to predict primary combined endpointss

	Univariable Cox proportional hazards regression		Multivariable Cox proportional hazards regression	
	HR(95% CI)	*p-value*	HR(95% CI)	*p-value*
LVEF (%)	0.963(0.941, 0.985)	0.001*	0.986(0.957, 1.016)	0.351
IC%	1.009(0.991, 1.026)	0.330	——	——
IBZ%	1.008(0.992, 1.024)	0.328	——	——
BZ entropy	2.315(1.531, 3.500)	<0.001*	1.708(0.943, 3.095)	0.078
IC entropy	2.045(1.264, 3.308)	0.004*	0.710(0.412, 1.225)	0.219
IBZ entropy	1.428(1.966, 2.109)	0.074	——	——
LV entropy	1.238(0.951, 1.615)	0.113	——	——
GRS(%)	0.972(0.945, 1.001)	0.059	——	——
GCS(%)	0.987(0.956, 1.019)	0.424	——	——
GLS(%)	0.946(0.901, 0.994)	0.026*	1.059(0.927, 1.209)	0.401
LVMD(ms)	1.019(1.012,1.027)	<0.001*	1.014(1.003, 1.024)	0.010*

*$p<0.05$ is accepted as statistically significant

LVEF, left ventricular ejection fraction; BZ, border zone; IC, infarct zone; IBZ, infarct zone and border zone; GRS, global radial strain; GCS, global circumferential strain; GLS, global longitudinal strain; LVMD, left ventricular mechanical dispersion

Prognosis eveluation

Over a mean follow-up of 31 months, primary combined endpoints occurred in 42 of the 181 participants, 6 were SCD, 24 experienced VAs or/and received ICD therapy for VAs, and 12 suffered from new CHF. ROC results were showed in Table 3. According to the results of Delong test, the performance of LVMD and BZ entropy were significantly superior to other parameters ($p<0.05$ for all) for primary combined endpoints prediction, whereas LVMD is not better than BZ entropy ($p=0.344$).

Table 4 provides the results of univariate and multivariate Cox regression analysis for primary combined endpoints predicting. LVEF [hazard ratio (HR): 0.963; 95% confidence interval (CI): 0.941, 0.985; $p=0.001$], BZ entropy (HR: 2.315; 95% CI: 1.531, 3.500; $p<0.001$), IC entropy (HR: 1.009; 95% CI: 0.991, 1.026; $p=0.004$), GLS (HR: 0.946; 95% CI: 0.901, 0.994; $p=0.026$) and LVMD (HR: 1.019; 95% CI: 1.012, 1.027; $p<0.001$) were correlated with possibility of primary combined endpoints in all patients. Collinearity diagnostics were conducted to avoid the confounding effect of the correlation between two entropy-related indexes (BZ entropy and IC entropy). The results demonstrated no collinearity between them (VIF=1). After adjusting for LVEF, BZ entropy, IC entropy, and GLS, LVMD was still identified as an independent predictor for primary combined endpoints (HR: 1.014; 95% CI: 1.003, 1.024; $p=0.010$). A Kaplan-Meier survival curve was drawn for patients with LVMD≤cut-off value (86.955ms) versus LVMD>86.955ms, and the analysis provided significant evidence of an increased risk of primary combined endpoints among patients with high LVMD ($p<0.001$, log-rank) (Fig. 4). The prediction model combining LVMD, BZ entropy with LVEF had an AUC value of 0.871 in predicting primary combined endpoints after MI, which was superior to single LVEF ($p=0.002$, Delong test).

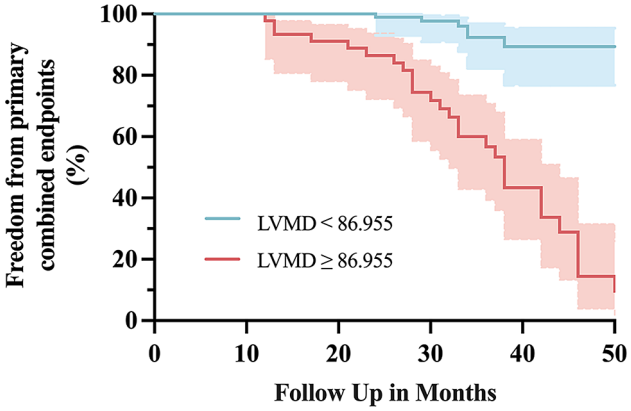

Fig. 4 Kaplan-Meier survival curve of patients with LVMD ≤ cut-off value (86.955ms) versus LVMD > cut-off value (86.955ms). Patients with higher LVMD were more likely to occurrence at primary combined endpoints ($p < 0.001$, log-rank)

Discussion

Survivors of MI have a high risk of SCD because of the elevated long-term incidence of fatal advers cardiovascular events [14]. Myocardial fibrosis formation is a process of remodeling of infarcted myocardium, with structural and electrophysiological remodeling occurring within the scar, reflected in increased heterogeneity. The post-MI myocardium, composed of an intermingling of cardiomyocytes and fibrotic bundles, remains electrophysiologically active and can contribute to abnormal cardiac electrical activity [15]. In this study, we retrospectively collected post-MI patients and the prognostic value of two types of parameters reflecting heterogeneity was explored. The main findings are as follows: (A) LGE entropy and LVMD effectively reflect post-MI myocardial heterogeneity, and the correlations between them have been substantiated. (B) LVMD have shown superior predictive efficacy for primary combined endpoints compared to traditional recommendation parameter LVEF. (C) The prediction model integrating LVMD, BZ entropy, and LVEF demonstrated strong performance in forecasting primary combined endpoints after MI.

Myocardial ischemic injury, accompanied by secondary fibrosis, induces heterogeneity in electrical conduction at the ventricular level and exacerbates electro-mechanical dyssynchrony [16]. LVMD can reflect these changes, a cross-sectional study conducted in 2021 explored the relationship between electrocardiographic conduction and myocardial longitudinal strain parameters in a normal population and demonstrated a significant nonlinear relationship between most myocardial electrophysiologic indices and LVMD, suggesting that LVMD may reflect heterogeneity in myocardial electrophysiologic activity [17]. The larger the LVMD value is, the longer the myocardial electrical conduction time and the larger the electrical dispersion is.

Myocardial electrophysiologic heterogeneity can cause myocardial contractional heterogeneity, resulting from regional differences in electrical conduction properties, primarily in slow conduction regions [17]. LVMD can evaluate contractional heterogeneity and has been proven to be a marker of electrophysiologic heterogeneity including inhomogeneous anisotropy, electrolytic coupling, conduction block, and slow conduction [18]. The results of the present study showed correlations between all 4 entropy parameters (BZ, IC, IBZ, and LV entropy) and LVMD, with the highest correlation found for the BZ entropy. According to previous evidence, structural heterogeneity between fibrotic myocardium and surviving myocardium within specific areas — the BZ — leads to uneven contraction, explaining the correlation between these two parameters [19]. Structural heterogeneity occurs after MI as a result of the reduction of normal cardiomyocytes and the development of myocardial fibrosis. Results in changes in ventricular load force and regional wall stress, that is myocardial contractility and relaxation capacity after MI [20]. This may affect the formation of depolarizing and repolarizing abnormal impulses and can lead to electrophysiological heterogeneity [21]. Structural heterogeneity is present and quantifiable in MI-involved myocardium and is associated with increased ventricular irritability with programmed electrical stimulation [22]. Thus, it can be broadly considered correlations between structural heterogeneity and electrophysiological heterogeneity.

Survivors of MI are at risk of recurrent cardiovascular events, with a morbidity of 12% within 6 months [23]. SCD, sustained VA, ICD implantation, and HF regarding primary combined endpoints in the present study are considered very important severe adverse outcomes. VA are usually caused by re-entry mechanisms and BZ is the pivotal substrate. Heterogeneous and slow conduction in BZ, where activation proceeds along the pathway-branching and merging of surviving myocardial bundles separated by collagen septal lengthen the pathway, a key condition for the occurrence of re-entry [24]. In a multicenter study of 7-year follow-up in patients with HF, the incidence of in-hospital sustained VA was 4.2% [25].

ROC analysis results have shown LVMD and entropy are more effective parameters for evaluating prognosis compared to traditional LVEF. Therefore, they are recommended for predicting primary combined endpoints. Our study has demonstrated that entropy correlates with primary combined endpoints in MI, aligning with findings from previous research. The results of a study in post-MI patients showed that IBZ entropy was independently associated with VAs and was the only CMR parameter associated with appropriate ICD therapy [5]. A study of sustained VA prediction in hypertrophic cardiomyopathy (HCM) patients in 2021 demonstrated that entropy

allows risk stratification of VAs [27]. In 2022, Antiochos demonstrated that entropy was independently associated with primary combined endpoints after adjusting LVEF, QRS time frame, and LGE% in VA patients [28]. For the research, entropy has a higher prognostic value than LVEF and LGE%, and BZ entropy has the highest prognostic predictive value.

Another advantage is that entropy is calculated using the standard algorithm, which makes it more reproducible for both intra- and inter- observers' measurements. Thus, entropy may offer a realistic and robust method of primary combined endpoints risk assessment. However, there are no sufficient prospective randomized studies with definitive conclusions as to which entropy parameter is superior. The present cohort study defined the structural heterogeneity of BZ in terms of entropy and showed that BZ entropy could be used as a predictive parameter of primary combined endpoints with a higher accuracy than LVEF.

Another highlight of the study was the predictive value of CMR-determined LVMD for primary combined endpoints after MI. Experiments have shown that electrical remodeling occurs within the infarct 'limbic region', leading to slow conduction and facilitating re-entry [29]. The specific mechanisms of re-entry depend on the structural remodeling properties of BZ [30]. In 2022, a study on myocardial microstructure confirmed the presence of electrical conduction dysfunction following MI. Additionally, the BZ was identified as the predominant source of post-MI sustained VA in mice [31].Therefore, accurate mechanical and electrical characterization of BZ is crucial for improving the prognosis of patients with MI [32].

The results of a meta-analysis showed that LVMD is a marker of electrophysiological heterogeneity and contributes to sustained VA [18]. Patients with prolonged LVMD demonstrated inhomogeneous electrical conduction and provided the highest predictive value for the primary combined endpoints. In 2020, a total of 1,000 patients with MI undergoing primary PCI were prospectively analyzed. After a median follow-up of 117 months, an increase in LVMD determined by CMR was independently associated with an increased risk of all-cause mortality [33]. In addition to the proven value of LVMD in patients with MI, LVMD has important prognostic value in other cardiac conditions as well. The results of a study in the general population indicated that both systolic and diastolic dysfunction were associated with LVMD and coronary artery disease, hypertension, diabetes mellitus, and obesity were more common in subjects with higher LVMD [34]. Regardless of etiology, the use of LVEF alone to predict sustained VA and SCD is less effective, especially in patients with moderately reduction. LVMD improves prognosis assessment, especially in patients currently excluded from ICD placement based on LVEF [35].

According to a HCM study in 2015, LVMD was associated with the presence of sustained VA, and LVMD improved risk stratification for HCM [36]. In addition, LVMD may contribute to the prognostic stratification of HF patients and is associated with a poor prognosis in those with severely reduced LV function and bundle branch conduction block [37]. Higher LVMD at follow-up in patients with HF was associated with sustained VA independent of whether final LVEF was below or above the guideline-reported 35% cut-off. Although the risk of sustained VA was significantly reduced in patients whose LVEF improved to >35% at follow-up, it remained elevated in the presence of an elevated LVMD [38]. For different studies and different subject populations, the cut-off value of LVMD for primary combined endpoints prediction varies widely and reported to have a wide range between 47ms-221ms [8]. For our study, the cutoff value of LVMD for primary combined endpoints prediction was 86.955ms.

Theoretically, assessing myocardial heterogeneity offers significant clinical value for patients who experience primary combined endpoints following MI. However, limited research has explored myocardial heterogeneity in depth. This study is the first to develop an evaluation model utilizing CMR heterogeneity parameters. By integrating LVEF, BZ entropy, andLVMD, our prediction model outperforms LVEF alone in predicting primary combined endpoints after MI. We propose that this model supplements and enhances the current guidelines and reference evaluation system. CMR has gained widespread international recognition and adoption in clinical practice due to its unparalleled ability to visualize cardiac tissues non-invasively and without exposure to ionizing radiation. Researches have demonstrated the clinical value and risk prediction benefit of CMR parameters on patients after MI. At the same time, with the advancement of scanning technology and computer aided technology, the scanning time is shortened and post-processing simplification. All of the above can improve the clinical application value of CMR in long-term evaluation of patients after MI and the possibility of follow-up on a large scale.

Our study has several limitations. It is a single-center, observational study with a relatively small sample size. The definition of primary combined endpoints included a combination of SCD, sustained VA or/and ICD implantation, and new HF. Due to the limited sample size, we are unable to further discuss the specific events at different endpoints. While the results indicate that LVMD is linearly related to entropy parameters, the correlation coefficient is small, and the accuracy of these findings requires further investigation. Another limitation is that

we did not compare the LVMD measurements obtained by CMR with those obtained by echocardiography.

Conclusions

Myocardial heterogeneity measured with CMR-derived LVMD and entropy are readily available and reproducible parameters reflecting cardiac remodeling after MI, which have the potential to be applied to primary combined endpoints prediction for post-MI patients. A linear correlation has been observed between LVMD and entropy, but the correlation coefficient is relatively small and requires further validation. LVMD has independent prognostic value, and LVMD combining with the guideline-recommended LVEF as a united model escalates the forecast accuracy of primary combined endpoints' risk in patients after MI. Considering the limitations of this study, further studies are needed to investigate the association between LVMD, entropy, and adverse outcomes after MI.

Author contributions

Xiaoying Zhao: Conceptualization, methodology and original manuscript. Li Zhang: Methodology, formal analysis and visualization. Lujing Wang: Software and validation. Wanqiu Zhang: Data Curation and formal analysis. Yujiao Song: Data Curation. Xinxiang Zhao: Review and editing, funding acquisition. Yanli Li: Supervision.

Funding

United Fund of Yunnan Provincial Science and Technology Department and Kunming medical University 202201AY070001-097. Yunnan Science and Technology Platform and Talent Project (Academician Expert Workstation) 202305AF150033. Multicenter Ischemic Heart Disease Research in Yunnan Province YXJL-2022-0665-0214.

Data availability

No datasets were generated or analysed during the current study.

Declarations

Ethics approval and consent to participate

This study was conducted in accordance with the principles of the Helsinki. The studies involving human participants were reviewed and approved by the Institutional Review Committee of The Second Affiliated Hospital of Kunming Medical University.

Consent for publication

Not applicable.

Competing interests

The authors declare no competing interests.

Author details

[1]Department of Radiology, The Second Affiliated Hospital of Kunming Medical University, Dianmiandadao No. 374, Kunming, Yunnan 650101, China
[2]Department of Radiology, Qujing No.1 Hospital, Kirin District Garden Road no. 1, Qujing 655099, China

Received: 4 July 2024 / Accepted: 24 December 2024
Published online: 04 January 2025

References

1. Ma LY, Wang ZW, Fan J, Hu ZS. Chinese cardiovascular health and disease report 2022 points. China Gen Med. 2023;26(32):3975–94.
2. Amoni M, Dries E, Ingelaere S, Vermoortele D, Roderick HL, Claus P, et al. Ventricular arrhythmias in ischemic cardiomyopathy-new avenues for mechanism-guided treatment. Cells. 2021;10:2629.
3. Dickfeld T, Field ME, Fonarow GC, Gillis AM, Granger CB, Hammill SC, et al. 2017 AHA/ACC/HRS guideline for management of patients with ventricular arrhythmias and the prevention of sudden cardiac death: a report of the American College of Cardiology/American Heart Association Task Force on Clinical Practice guidelines and the Heart Rhythm Society. J AM COLL CARDIOL. 2018;72(14):91–220.
4. Hall TS, von Lueder TG, Zannad F, Rossignol P, Duarte K, Chouihed T, et al. Relationship between left ventricular ejection fraction and mortality after myocardial infarction complicated by heart failure or left ventricular dysfunction. Int J Cardiol. 2018;272(10):260–6.
5. Androulakis AFA, Zeppenfeld K, Paiman EHM, Piers SRD, Wijnmaalen AP, Siebelink HJ, et al. Entropy as a Novel measure of myocardial tissue heterogeneity for prediction of ventricular arrhythmias and mortality in Post-infarct patients. JACC Clin Electrophysiol. 2019;5(4):480–9.
6. Zegard A, Okafor O, de Bono J, Kalla M, Lencioni M, Marshall H, et al. Greyzone myocardial fibrosis and ventricular arrhythmias in patients with a left ventricular ejection fraction > 35. Europace. 2022;24(1):31–9.
7. Bertini M, Schalij MJ, Bax JJ, Delgado V. Emerging role of multimodality imaging to evaluate patients at risk for sudden cardiac death. Circ Cardiovasc Imaging. 2012;5(4):525–35.
8. Abou R, Prihadi EA, Goedemans L, van der Geest R, El Mahdiui M, Schalij MJ, et al. Left ventricular mechanical dispersion in ischaemic cardiomyopathy: association with myocardial scar burden and prognostic implications. Eur Heart J Cardiovasc Imaging. 2020;21(11):1227–34.
9. Muser D, Tioni C, Shah R, Selvanayagam JB, Nucifora G. Prevalence, correlates, and prognostic relevance of myocardial mechanical dispersion as assessed by feature-tracking Cardiac magnetic resonance after a First ST-Segment Elevation myocardial infarction. Am J Cardiol. 2017;120(4):527–33.
10. Haland TF, Almaas VM, Hasselberg NE, Saberniak J, Leren IS, Hopp E, et al. Strain echocardiography is related to fibrosis and ventricular arrhythmias in hypertrophic cardiomyopathy. Eur Heart J Cardiovasc Imaging. 2016;17(6):613–21.
11. Zeppenfeld K, Tfelt-Hansen J, de Riva M, Winkel BG, Behr ER, Blom NA, et al. 2022 ESC guidelines for the management of patients with ventricular arrhythmias and the prevention of sudden cardiac death. Eur Heart J. 2022;43(4):3997–4126.
12. Zhang Y, Zhu Y, Wang D, Xu L, Jiang W, Wang J, et al. Cardiac index: a superior parameter of cardiac function than left ventricular ejection fraction in risk stratification of hypertrophic cardiomyopathy. Heart Rhythm. 2023;20(7):958–67.
13. Cui JL, Wen CY, Hu Y, Li TH, Luk KD. Entropy-based analysis for diffusion anisotropy mapping of healthy and myelopathic spinal cord. NeuroImage. 2011;54(3):2125–31.
14. Sarter BH, Finkle JK, Gerszten RE, Buxton AE. What is the risk of sudden cardiac death in patients presenting with hemodynamically stable sustained ventricular tachycardia after myocardial infarction? J AM COLL CARDIOL. 1996;28(1):122–9.
15. De Jong S, Van Rijen H, De Bakker J. Fibrosis and Cardiac Arrhythmias. J Cardiovasc Pharmacol. 2011;57(6):630–8.
16. Akazawa Y, Fujioka T, Yazaki K, Strbad M, Horer J, Kuhn A, et al. Right ventricular electromechanical Dyssynchrony and its relation to right ventricular remodeling, dysfunction, and Exercise Capacity in Ebstein Anomaly. J Am Soc Echocardiogr. 2023;36(6):634–43.
17. Groeneveld SA, van der Ree MH, Taha K, de Bruin-Bon RHA, Cramer MJ, Teske AJ, et al. Echocardiographic deformation imaging unmasks global and regional mechanical dysfunction in patients with idiopathic ventricular fibrillation: a multicenter case-control study. Heart Rhythm. 2021;18(10):1666–72.
18. Kawakami H, Nerlekar N, Haugaa KH, Edvardsen T, Marwick TH. Prediction of ventricular arrhythmias with left ventricular mechanical dispersion: a systematic review and Meta-analysis. JACC Cardiovasc Imaging. 2020;13(2):562–72.
19. Hegyi B, Bossuyt J, Griffiths LG, Shimkunas R, Coulibaly Z, Jian Z, et al. Complex electrophysiological remodeling in postinfarction ischemic heart failure. Proc Natl Acad Sci U S A. 2018;115(13):e3036–44.
20. Podlesnikar T, Pizarro G, Fernandez-Jimenez R, Montero-Cabezas JM, Greif N, Sanchez-Gonzalez J, et al. Left ventricular functional recovery of infarcted and remote myocardium after ST-segment elevation myocardial infarction

(METOCARD-CNIC randomized clinical trial substudy). J Cardiovasc Magn Reson. 2020;22(1):44.
21. Ashikaga H, Mickelsen SR, Ennis DB, Rodriguez I, Kellman P, Wen H, et al. Electromechanical analysis of infarct border zone in chronic myocardial infarction. AM J PHYSIOL-HEART C. 2005;289(3):1099–105.
22. Schmidt A, Azevedo CF, Cheng A, Gupta SN, Bluemke DA, Foo TK, et al. Infarct tissue heterogeneity by magnetic resonance imaging identifies enhanced cardiac arrhythmia susceptibility in patients with left ventricular dysfunction. Circulation. 2007;115(15):2006–14.
23. Ibanez B, James S, Agewall S, Antunes MJ, Bucciarelli-Ducci C, Bueno H, et al. 2017 ESC guidelines for the management of acute myocardial infarction in patients presenting with ST-segment elevation:the Task Force for the management of acute myocardial infarction in patients presenting with ST-segment elevation of the European Society of Cardiology (ESC). Eur Heart J. 2018;39(2):119–77.
24. de Bakker JM, van Capelle FJ, Janse MJ, Tasseron S, Vermeulen JT, de Jonge N. Slow Conduction Infarcted Hum Heart 'Zigzag'CourseofActivation Circulation. 1993;88(3):915–26.
25. Roe AT, Ruud M, Espe EK, Manfra O, Longobardi S, Aronsen JM, et al. Regional diastolic dysfunction in post-infarction heart failure: role of local mechanical load and SERCA expression. Cardiovasc Res. 2019;115(4):752–64.
26. Alenazy B, Tharkar S, Kashour T, Alhabib KF, Alfaleh H, Hersi A. In-hospital ventricular arrhythmia in heart failure patients: 7 year follow-up of the multicentric HEARTS registry. ESC Heart Fail. 2019;6(6):1283–90.
27. Ye Y, Ji Z, Zhou W, Pu C, Li Y, Zhou C, et al. Mean Scar Entropy by Late Gadolinium Enhancement Cardiac magnetic resonance is Associated with ventricular arrhythmias events in hypertrophic cardiomyopathy. Front Cardiovasc Med. 2021;8(11):758635.
28. Antiochos P, Ge Y, van der Geest RJ, Madamanchi C, Qamar I, Seno A, et al. Entropy as a measure of myocardial tissue heterogeneity in patients with ventricular arrhythmias. JACC Cardiovasc Imaging. 2022;15(5):783–92.
29. Yao JA, Hussain W, Patel P, Peters NS, Boyden PA, Wit AL. Remodeling of gap junctional channel function in epicardial border zone of healing canine infarcts. Circ Res. 2003;92(4):437–43.
30. Mendonca Costa C, Plank G, Rinaldi CA, Niederer SA, Bishop MJ. Modeling the electrophysiological properties of the Infarct Border Zone. Front Physiol. 2018;9(4):356.
31. Zhu C, Rajendran PS, Hanna P, Efimov IR, Salama G, Fowlkes CC, et al. High-resolution structure-function mapping of intact hearts reveals altered sympathetic control of infarct border zones. JCI Insight. 2022;7(3):e153913.
32. Liang C, Li Q, Wang K, Du Y, Wang W, Zhang H. Mechanisms of ventricular arrhythmias elicited by coexistence of multiple electrophysiological remodeling in ischemia: a simulation study. PLoS Comput Biol. 2022;18(4):e1009388.
33. Abou R, Goedemans L, van der Bijl P, Fortuni F, Prihadi EA, Mertens B, et al. Correlates and long-term implications of left ventricular mechanical dispersion by two-Dimensional Speckle-Tracking Echocardiography in patients with ST-Segment Elevation myocardial infarction. J Am Soc Echocardiogr. 2020;33(8):964–72.
34. Aagaard EN, Kvisvik B, Pervez MO, Lyngbakken MN, Berge T, Enger S, et al. Left ventricular mechanical dispersion in a general population: data from the Akershus Cardiac Examination 1950 study. Eur Heart J Cardiovasc Imaging. 2020;21(2):183–90.
35. Kosiuk J, Dinov B, Bollmann A, Koutalas E, Mussigbrodt A, Sommer P, et al. Association between ventricular arrhythmias and myocardial mechanical dispersion assessed by strain analysis in patients with nonischemic cardiomyopathy. Clin Res Cardiol. 2015;104(12):1072–7.
36. Popa-Fotea NM, Micheu MM, Onciul S, Zamfir D, Dorobantu M. Combined right and left ventricular mechanical dispersion enhance the arrhythmic risk stratification in hypertrophic cardiomyopathy. J Cardiol. 2020;76(4):364–70.
37. Stankovic I, Janicijevic A, Dimic A, Stefanovic M, Vidakovic R, Putnikovic B, et al. Mechanical dispersion is associated with poor outcome in heart failure with a severely depressed left ventricular function and bundle branch blocks. Ann Med. 2018;50(2):128–38.
38. Carluccio E, Biagioli P, Mengoni A, Zuchi C, Lauciello R, Jacoangeli F, et al. Burden of ventricular arrhythmias in Cardiac Resynchronization Therapy Defibrillation and Implantable Cardioverter-Defibrillator recipients with recovered left ventricular ejection fraction: the additive role of Speckle-Tracking Echocardiography. J Am Soc Echocardiogr. 2022;35(4):355–65.

Publisher's note